SAE TECHNICAL PAPER SERIES

2006-01-0697

New Capabilities for the Virtual-Human Santos™

J. Yang, T. Marler, S. Beck, J. Kim, Q. Wang, X. Zhou, E. Pena Pitarch, K. Farrell, A. Patrick, J. Potratz, K. Abdel-Malek and J. Arora
The University of Iowa

Kyle Nebel
U.S. Army TACOM/RDECOM

Reprinted From: Military Vehicles (SP-2040)

ISBN 0-7680-1631-2

9 780768 016314

2006 World Congress
Detroit, Michigan
April 3-6, 2006

SAE International™

400 Commonwealth Drive, Warrendale, PA 15096-0001 U.S.A. Tel: (724) 776-4841 Fax: (724) 776-0790 Web: www.sae.org

Report Documentation Page

Form Approved
OMB No. 0704-0188

1. REPORT DATE	2. REPORT TYPE	3. DATES COVERED
APR 2006		**00-00-2006 to 00-00-2006**

4. TITLE AND SUBTITLE	5a. CONTRACT NUMBER
New Capabilities for the Virtual-Human SantosTM	5b. GRANT NUMBER
	5c. PROGRAM ELEMENT NUMBER
6. AUTHOR(S)	5d. PROJECT NUMBER
	5e. TASK NUMBER
	5f. WORK UNIT NUMBER
7. PERFORMING ORGANIZATION NAME(S) AND ADDRESS(ES) **University of Iowa,Center for Computer Aided Design ,Vrtual Sodier Research Program,Iowa City,IA,52242**	8. PERFORMING ORGANIZATION REPORT NUMBER
9. SPONSORING/MONITORING AGENCY NAME(S) AND ADDRESS(ES)	10. SPONSOR/MONITOR'S ACRONYM(S)
	11. SPONSOR/MONITOR'S REPORT NUMBER(S)

12. DISTRIBUTION/AVAILABILITY STATEMENT
Approved for public release; distribution unlimited

13. SUPPLEMENTARY NOTES

14. ABSTRACT

This paper presents new capabilities of the virtual-human SantosTM introduced last year. SantosTM is an avatar that has extensive modeling and simulation features. It is a digital human model with over 100 degrees-of-freedom (DOF), where the hand model has 25 DOF, direct optimization-based method, and real-human like appearance. The newly developed analysis includes (1) a 25-DOF hand model that is the first step to study hand grasping; (2) posture prediction advances such as multiple end-effectors (two arms, two arms + head + legs), real-time inverse kinematics for posture prediction for any points, vision functionality; (3) dynamic motion prediction with external loads; and (4) musculosteletal modeling that includes determining muscle forces, and muscle stress. With these newly developed capabilities SantosTM can be used to test the joystick design, study grasping, facilitate vehicle interior design, test visibility for product design, predict correct dynamic motion or posture subject to external loads, and investigate muscle forces, and muscle stress. Finally, additional ongoing projects are summarized.

15. SUBJECT TERMS

16. SECURITY CLASSIFICATION OF:			17. LIMITATION OF ABSTRACT	18. NUMBER OF PAGES	19a. NAME OF RESPONSIBLE PERSON
a. REPORT **unclassified**	b. ABSTRACT **unclassified**	c. THIS PAGE **unclassified**	**Same as Report (SAR)**	**16**	

All SAE papers, standards, and selected books are abstracted and indexed in the Global Mobility Database.

ISSN 0148-7191

SAE TECHNICAL PAPER SERIES

2006-01-0697

New Capabilities for the Virtual-Human Santos™

J. Yang, T. Marler, S. Beck, J. Kim, Q. Wang, X. Zhou, E. Pena Pitarch, K. Farrell, A. Patrick, J. Potratz, K. Abdel-Malek and J. Arora
The University of Iowa

Kyle Nebel
U.S. Army TACOM/RDECOM

Reprinted From: Military Vehicles (SP-2040)

ISBN 0-7680-1631-2

9 780768 016314

2006 World Congress
Detroit, Michigan
April 3-6,2006

SAE International™

400 Commonwealth Drive, Warrendale, PA 15096-0001 U.S.A. Tel: (724) 776-4841 Fax: (724) 776-0790 Web: www.sae.org

All SAE papers, standards, and selected books are abstracted and indexed in the Global Mobility Database.

ISSN 0148-7191

2006-01-0697

New Capabilities for the Virtual-Human Santos™

J. Yang, T. Marler, S. Beck, J. Kim, Q. Wang, X. Zhou, E. Pena Pitarch, K. Farrell, A. Patrick, J. Potratz, K. Abdel-Malek and J. Arora
The University of Iowa

Kyle Nebel
U.S. Army TACOM/RDECOM

ABSTRACT

This paper presents new capabilities of the virtual-human Santos™ introduced last year. Santos™ is an avatar that has extensive modeling and simulation features. It is a digital human model with over 100 degrees-of-freedom (DOF), where the hand model has 25 DOF, direct optimization-based method, and real-human like appearance. The newly developed analysis includes (1) a 25-DOF hand model that is the first step to study hand grasping; (2) posture prediction advances such as multiple end-effectors (two arms, two arms + head + legs), real-time inverse kinematics for posture prediction for any points, vision functionality; (3) dynamic motion prediction with external loads; and (4) musculosteletal modeling that includes determining muscle forces, and muscle stress. With these newly developed capabilities Santos™ can be used to test the joystick design, study grasping, facilitate vehicle interior design, test visibility for product design, predict correct dynamic motion or posture subject to external loads, and investigate muscle forces, and muscle stress. Finally, additional ongoing projects are summarized.

Keywords: Virtual humans, direct optimization-based approach, human performance measures.

INTRODUCTION

The development of realistic virtual (computer-based) humans is quickly gaining momentum in the research arena as well as in the industry and military sectors. There are several commercial products available such as Ramsis®, Jack®, Safework®, Realman®, etc. None of them has been developed using the direct optimization-based approach. In last year's report we presented the new generation of virtual humans (Santos™). This paper will introduce newly developed capabilities of Santos™.

There are essentially three stages to developing virtual humans: (1) basic human modeling, (2) input functionality, and (3) intelligent reaction to input (memory, reasoning, etc.). This paper and last year's report address developments in the first stage of virtual humans. The ultimate goal will be towards the second and third stages.

This paper presents the newly developed capabilities for Santos™ that entails hand modeling; posture prediction with multiple end-effectors; inverse kinematics (IK); a vision objective function, and self-collision avoidance; motion prediction with external loads; and musculoskeletal modeling.

HAND MODEL

A virtual human hand is an essential part of a virtual human's form, function, and communication, capable of complex, expressive articulation. There are considerable works on hand modeling. ElKoura and Singh (2003) categorized hand modeling as engaging several areas of research such as anatomy, robotics, animation industry, graphics and vision, and music. Wan *et al* (2004), and Savescu *et al* (2004) also developed different hand models. The hand's degrees of freedom (DOF) are from 21 to 27 for different research groups in the literature. Our objective is to develop a realistic hand model based on the work of previous researchers.

A human hand has 27 bones (Fig. 1). The symbolic Roman numbers are assigned for fingers: the thumb is I, the index finger is II, the middle finger is III, the ring finger is IV, and the little finger is V. At the base of each finger is one metacarpal bone, which connects to the wrist. Carpometacarpal (CMC) joints connect the metacarpal bones to the wrist. The CMC joints for II and III are static: they cannot actually rotate. In contrast, the CMC joints for I, IV, and V can rotate with Flexion/Extension (F/E) and Abduction/Adduction (Ab/Ad). The metacarpophalangeal (MCP) joints connect the metacarpal bones to the

the metacarpal bones to the phalanx bones. These MCP joints can also move with 2 DOF (F/E and Ab/Ad). An interphalangeal (IP) joint connects the two phalanx bones in the thumb and has one rotational degree of freedom. Proximal Interphalangeal (PIP) joints connect the two inner (not the tip) phalanxes in II, III, IV, and V. These joints have one rotational DOF in the F/E direction. The last joint is the distal interphalangeal (DIP) joint. It connects the fingertips, the final phalanxes in each of the fingers (II, III, IV, and V), and it moves in F/E direction.

From the above described anatomy, the hand can be modeled as 25 DOF shown in Fig. 2. All of joints in the hand are revolute joints.

Hand bones have different lengths for different fingers. All link lengths depend on two parameters HL and HB, where HL is the length of the hand, and HB is the width of the hand (Pena Pitarch *et al* 2005).

ADVANCES IN POSTURE PREDICTION

There are several approaches for posture prediction such as empirical approaches (Beck and Chaffin 1992; Berme *et al,* 1987; Das and Behara 1998; Faraway *et al,* 1999), inverse kinematic methods, in particular pseudo-inverse methods (Jung and Choe 1996; Jung *et al,* 1992; 1995; Kee *et al,* 1994), and the optimization-based method (Yang *et al,* 2004). It is important to consider multiple end-effectors, collision-free, and incorporated vision objective function in the optimization-based method for posture prediction.

In this section, we first provide a brief overview of our approach to posture prediction. We then discuss the basics of some of the latest developments of this area with respect to Santos™. Four key advancements are presented: 1) the ability to predict postures with restrictions on any number of end-effectors on the body, 2) an innovative version of human inverse kinematics, 3) a new performance measure that governs predicted postures based on one's ability to see an object, and 4) incorporation of self-avoidance, a capability that essentially makes Santos™ aware of his own body.

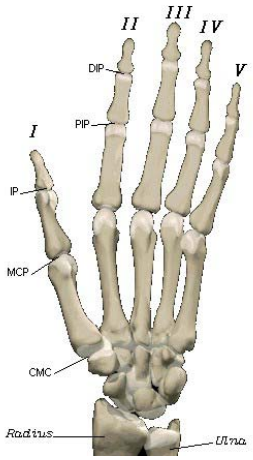

Fig. 1. Right hand with 5 rays (in a posterior view)

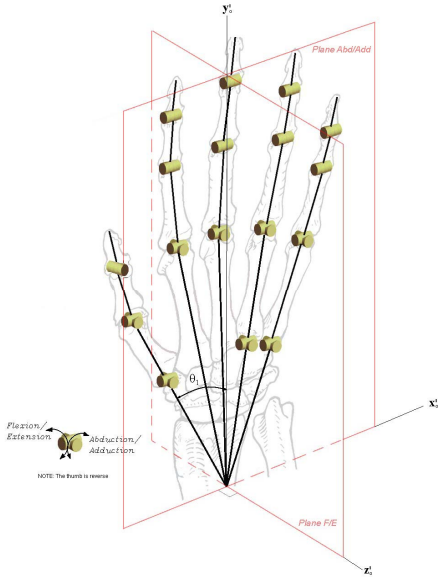

Fig. 2. Dorsal view right hand model

GENERAL APPROACH

Our direct optimization-based approach to posture prediction is summarized here, while Marler *et al* (2005a, 2005b) provide details. This approach involves finding the joint angles, **q**, in order to minimize one or more human performance measures that serve as the objective functions and govern posture. The problem is constrained by limits on the joint angles and by the requirement that the avatar must contact the target point. The final optimization formulation is given as follows:

Find: $\mathbf{q} \in R^{DOF}$ (1)

to minimize: Human performance measure(s)

subject to: $\left[\mathbf{x}(\mathbf{q})^{end\text{-}effector} - \mathbf{x}^{target\ point}\right]^2 \le \varepsilon$

$q_i^L \le q_i \le q_i^U;\ i = 1, 2, \ldots, DOF$

This problem is solved numerically using the software SNOPT (Gill *et al*, 2002), which uses sequential quadratic programming (Arora, 2004). Details concerning the different components of the optimization formulation are discussed as follows.

The design variables are the generalized coordinates q_i, which represent the components of the vector **q**. These design variables have units of radians. The first constraint in (1) is the *distance-constraint*, and it requires that the end-effector contact a predetermined target point in Cartesian space, where ε is a small positive number that approximates zero. In addition, each joint angle is constrained to lie between lower and upper limits, represented by q_i^L and q_i^U, respectively. These limits may be changed according to different sets of anthropologic data.

One of the most significant advantages of this approach is that it is completely predictive; it does not depend on predetermined data or prerecorded simulations. It thus affords the avatar a substantial amount of autonomy. In addition, this approach is relatively fast, providing results in real time. Finally, various capabilities and types of functionality can be incorporated simply by modifying or adding different performance measures and/or constraints. For instance, multiple end-effectors can be modeled with additional constraints (Farrell *et al*, 2005). Orientation of various body parts can be specified with additional constraints as well (Yang *et al*, 2005). Ideas such as musculoskeletal discomfort can be modeled as a performance measure (Marler *et al*, 2005). In the following sections, we discuss how multiple end effectors and self-avoidance can also be incorporated as constraints, and how the effects of vision on posture can be studied using a new performance measure. Ultimately, these posture prediction capabilities serve as a component of dynamic motion prediction, which is discussed later in the paper.

MULTIPLE END-EFFECTORS

As suggested in Yang *et al* (2004), the DH-method is used to determine the Cartesian location of an end-effector, based on joint angles. This method can be used to determine the position of any point on the body. In fact, a user can specify any point(s) in space relative to any single local coordinate system(s). Such point(s) can then be constrained to contact any target point(s), by adding additional distance constraints in (1), as demonstrated in Fig. 3. This capability is used, for example, when Santos™ is required to have his elbows remain on armrests or his back remain against the back of a seat.

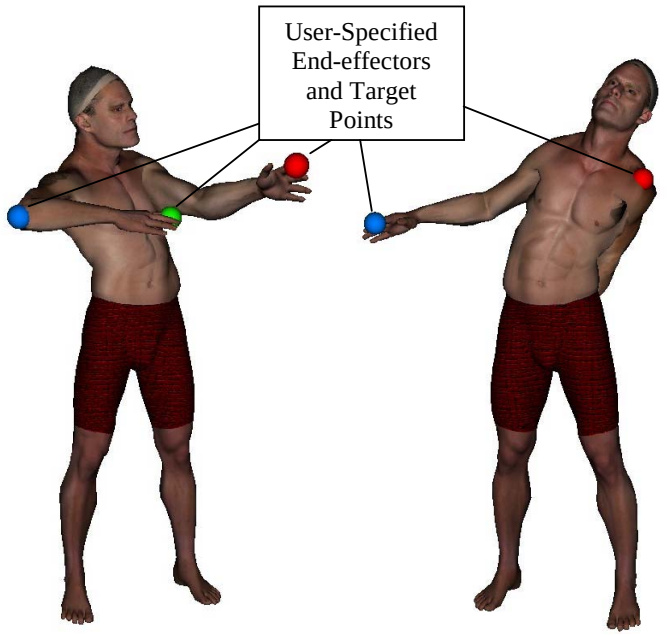

Fig. 3. Multiple End-effectors

ADVANCED INVERSE KINEMTICS (IK)

Virtual humans are most commonly used as mannequins that can be positioned manually in a particular setting or in virtual prototype. It is crucial that Santos™ not lose this necessary functionality. To be sure, the predictive capabilities of Santos™ exceed those of currently available tools, nonetheless, a user must be able to position Santos™ easily. We have developed two versions of inverse kinematics (IK): *standard IK* and *advanced IK*. Especially in advanced IK, we incorporate joint range of motion, and the results not only include joint angles, but also entail the values of human performance measures in real-time.

With standard IK (used in Maya®), the user is able to select *hot points* on Santos™ and then place them wherever is necessary, as shown in Figs. 4 and 5. The complete avatar then moves accordingly, in real time. However, standard IK does not incorporate joint ranges of motion and sometimes it generates odd postures. Therefore, we extend direct optimization-based posture prediction to advanced IK.

With advanced IK, we capitalize on posture prediction capabilities to yield an exciting new tool. As the user moves the hot points, the consequent posture is automatically predicted/optimized. That is, a version of the posture prediction algorithm is run with every frame, using the hot points as target points. This version of posture prediction currently has been optimized for speed, and non-critical features have been omitted. The algorithm is able to run approximately 20 times per second. This alleviates the need for a user to predict realistic postures as he/she positions the avatar; realistic postures are actually predicted automatically.

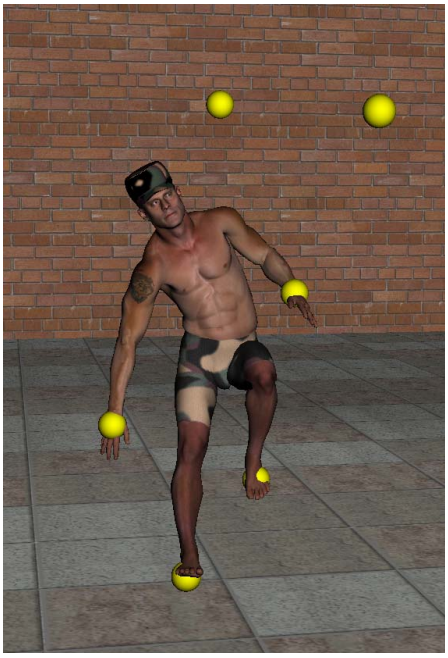

Fig. 4. Inverse Kinematics

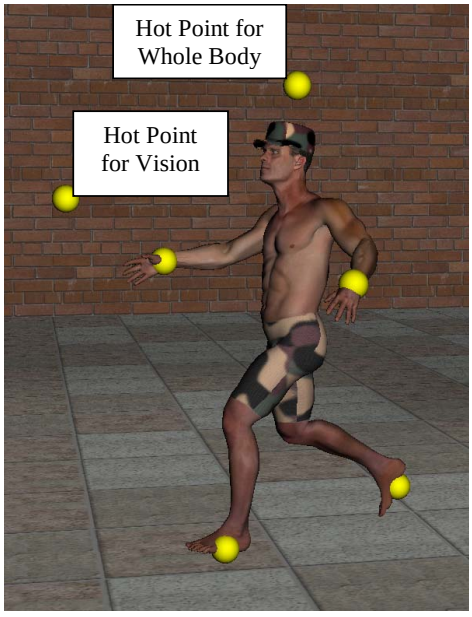

Fig. 5. Hot Points for Inverse Kinematics

PERFORMANCE MEASURE FOR VISION

Often, posture is governed by a natural desire to see the target one is striving to contact. This is demonstrated with Figs. 6a and 6b. Fig. 6a simply illustrates the posture that is achieved when musculoskeletal discomfort is minimized. Although the consequent posture is relatively comfortable in terms of joint stress, the avatar is apparently making no effort to see the target point, hence the motivation for modeling the effects of vision on posture.

This work with vision is an extension of the vision function developed by Kim *et al* (2004). It is based on visual acuity and essentially has three components. First, acuity is modeled as follows:

$$f_{acuity} = e^{-7(1-Cos\theta)^2} \quad (2)$$

where θ is the angle between the line of site and the line drawn directly from the avatar's head to the target point. In addition, a penalty function is added such that joint angles in the neck avoid their extreme limits. This complex penalty function is derived from the work by Marler *et al* (2005b). Finally, tilting of the head about the axis that projects outward orthogonal to the avatar's face, is minimized such that the corresponding DOF gravitate towards a neutral position.

SELF-COLLISION AVOIDANCE

A major concern with human modeling is the interaction between a human and his/her environment. Therefore, modeling self-collision avoidance and collision avoidance with environmental obstacles is crucial for realistic posture prediction. Obstacle avoidance with multi-body systems, such as robots, has been studied extensively (Ozaki and Mohri 1986; Kim and Khosla 1992; Kuffner *et al* 2002; and others). However, relatively little work has been done with human self-collision avoidance in the context of an optimization-based approach. We have implemented an approach with Santos™, where the self-collision avoidance capability is based on the Cartesian distances between different body parts. This distance is formulated as an additional distance constraint in (1). It requires that various end-effectors on the body do not collide with one another.

Fig. 6a. No Vision

Fig. 6b. With Vision

Using spheres with various sizes to represent different body parts, the self-collision avoidance constraints are expressed as follows:

$$\left[\mathbf{x}_i(\mathbf{q}) - \mathbf{x}_j(\mathbf{q})\right]^2 \geq \left(R_i + R_j\right)^2 \quad (3)$$

where $\mathbf{x}_i(\mathbf{q})$ and $\mathbf{x}_j(\mathbf{q})$ are the Cartesian coordinates of the centers of spheres *i* and *j* representing two body parts, and R_i and R_j are the radius of the two spheres, respectively. Distance-squared is implemented here instead of distance for the convenience of numerical calculations. An example of the effects of implementing the constraints in (3) is shown in Fig. 7, where a posture is compared with and without self-collision avoidance.

DYNAMIC MOTION PREDICTION

Dynamic motion prediction is a critical component for virtual humans. It can generate joint torques and predict joint injuries. Hase and Yamazaki (1997) simulated walking and rowing motion using muscle energy consumption formulas and human model, and the Newton-Euler method was used to calculate the joint torques. Chaffin (1997) developed two- and three-dimensional computerized human models for simulation of static strength during work. This paper reports on the development of an optimization-based dynamic motion prediction method.

Fig. 7. Posture prediction with self-collision avoidance

The general optimization-based method is defined as follows:

Find: Control Points ($P_{i,j} \quad i = 1,...,m;\ j = 1,...,n$)

to minimize: Metabolic Energy ($E_{Metabolic}$)

subject to:

Joint limits ($q_i^L \leq q_i \leq q_i^U \quad i = 1,...,n$)

Torque limits ($\tau_i^L \leq \tau_i \leq \tau_i^U \quad i = 1,...,n$)

Path constraints ($\| \mathbf{x}(\mathbf{q}(t)) - \mathbf{p}(t) \| \leq \varepsilon$)

Equations of motion

$$\left(\boldsymbol{\tau} = \mathbf{M}(\mathbf{q})\ddot{\mathbf{q}} + \mathbf{V}(\mathbf{q},\dot{\mathbf{q}}) + \sum \mathbf{J}_i^{\mathrm{T}} m_i \mathbf{g} + \sum \mathbf{J}_k^{\mathrm{T}} \mathbf{F}_k + \mathbf{K}\left(\mathbf{q} - \mathbf{q}^N\right)\right)$$

where τ_i is the generalized torque of joint-*I*, $\mathbf{J}_i^T$ is the transpose of the Jacobian matrix. $\mathbf{v}_i(\mathbf{q},\dot{\mathbf{q}})$ is the Coriolis and Centrifugal vector:

$$\mathbf{V}_i(\mathbf{q},\dot{\mathbf{q}}) = \sum_{k=1}^{n}\sum_{l=1}^{n}\sum_{j=\max(i,k,l)}^{n} Tr\left(\frac{\partial {}^0\mathbf{T}_j(\mathbf{q})}{\partial q_k}\mathbf{I}_j\left[\frac{\partial {}^0\mathbf{T}_j(\mathbf{q})}{\partial q_i}\right]^T\right)\dot{q}_k\dot{q}_l$$

$i,k,l = 1,2,...,n$, M_{ik} is the (i,k) element of the mass-inertia matrix $\mathbf{M}(\mathbf{q})$ such that

$$M_{ik}(\mathbf{q}) = \sum_{j=\max(i,k)}^{n} Tr\left(\frac{\partial {}^0\mathbf{T}_j(\mathbf{q})}{\partial q_k}\mathbf{I}_j\left[\frac{\partial {}^0\mathbf{T}_j(\mathbf{q})}{\partial q_i}\right]^T\right)$$

$\mathbf{I}_j$ is the inertia matrix and is written as follows:

$$\mathbf{I}_i = \begin{bmatrix} \frac{-I_{xx}+I_{yy}+I_{zz}}{2} & -I_{xy} & -I_{xz} & m_i\bar{x}_i \\ -I_{xy} & \frac{I_{xx}-I_{yy}+I_{zz}}{2} & -I_{yz} & m_i\bar{y}_i \\ -I_{xz} & -I_{yz} & \frac{I_{xx}+I_{yy}-I_{zz}}{2} & m_i\bar{z}_i \\ m_i\bar{x}_i & m_i\bar{y}_i & m_i\bar{z}_i & m_i \end{bmatrix}$$

m_i is the mass of link-*i*; $(\bar{x}_i, \bar{y}_i, \bar{z}_i)$ is the location of the center of gravity of link-*i*, expressed in terms of *i*th coordinate frame (local frame); and $I_{xx},\ldots,I_{xy},\ldots$ are the moments/products-of-inertia of link-*i* with respect to the *i*th coordinate system. **K** is a diagonal matrix of elastic constants given as follows:

$$\mathbf{K} = \begin{bmatrix} k_1 & & \mathbf{0} \\ & \ddots & \\ \mathbf{0} & & k_n \end{bmatrix}_{n\times n}$$

Note that all of the variables are functions of time, i.e., $\boldsymbol{\tau} = \boldsymbol{\tau}(t)$, $\mathbf{F}_k = \mathbf{F}_k(t)$, and $\mathbf{q} = \mathbf{q}(t)$, with $k = 1,2,...,n$. The total human metabolic energy expenditure rate is the sum of mechanical power, heat rate, and BMR.

$$\dot{E}_{Metabolic} \approx \sum_{i=1}^{n}\left|\tau_i(t)\dot{q}_i(t)\right| + \sum_{i=1}^{n} h_m^i\left|\tau_i(t)\right| + \dot{B}$$

$$\dot{B} = 0.685W + 29.8 \quad \text{(Joule/second or Watt)}$$

where W (Kg) is the body mass.

The following example is to predict the motion of moving a 9 kg object on one hand from a given initial position to a given final position in 2 seconds using the 21-DOF Santos™ upper-body (from waist to right hand) model. (Fig. 8).

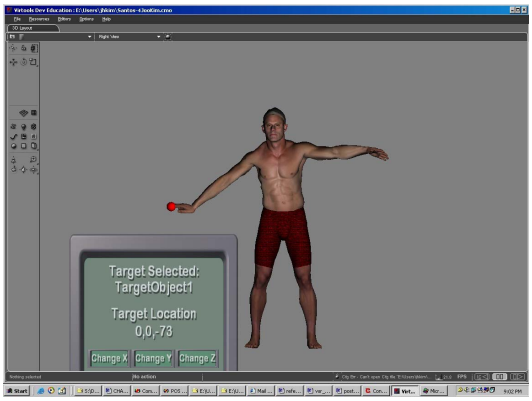

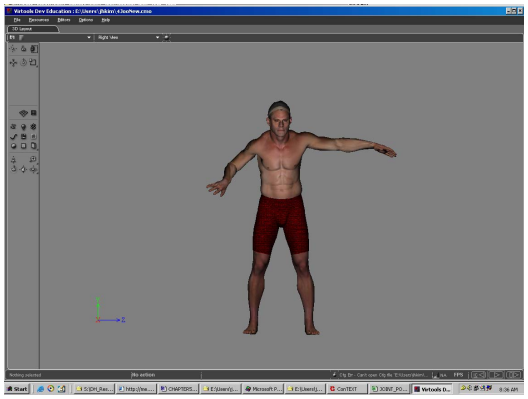

(a) At time t = 0 (initial) (b) At time t = 0.6

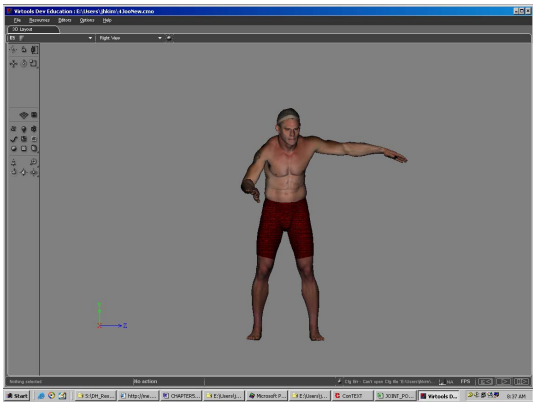

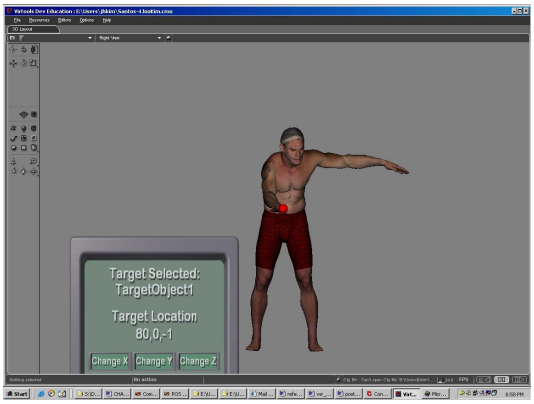

(c) At time t = 1.4 (d) at time t = 2 (final)

Fig. 8. Santos™ moving an object

The optimum joint kinematic profiles are obtained at each 0.04 of a second. The joint torque values are calculated and are recorded in Fig. 9. For intuitive validation of the above motion prediction, five human subjects were asked to perform the same task (with different object weights according to each subject's maximum capacity) and demonstrated similar motions. Fig. 10 shows the initial and final posture of a human subject.

In the initial posture, the spine joints for lateral bending exert large torques for right lateral bending, whereas in final posture, the spine joints for flexion/extension exert large torques for flexion. The large torque values for different motion segments will have different effects on the body and may cause different kinds of injury and injury risk levels (especially on the low-back). It can be observed that the initial and final postures have different distributions of the torques at the shoulder and arm joints. Although we have presented the initial validation work, systematic validation using more human subjects and the statistic method is ongoing.

MUSCULOSKELETAL MODELING

Through the understanding of simple mechanical principles and observing the anatomy of the human body, a model for predicting muscle forces to create desired joint torques is being developed for Santos™. Developing this model requires an understanding of the musculoskeletal system, the mechanical principles of how torque is generated through muscle tension, and optimization to solve the resulting indeterminate problem.

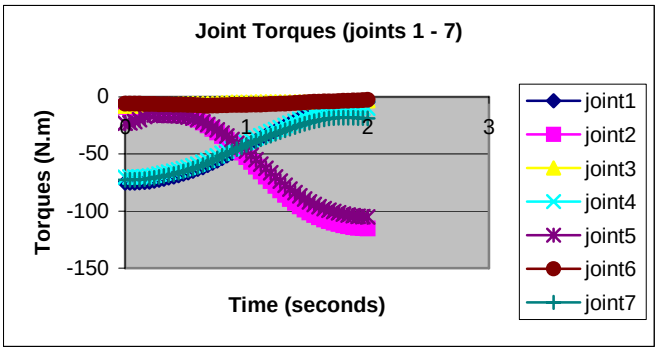

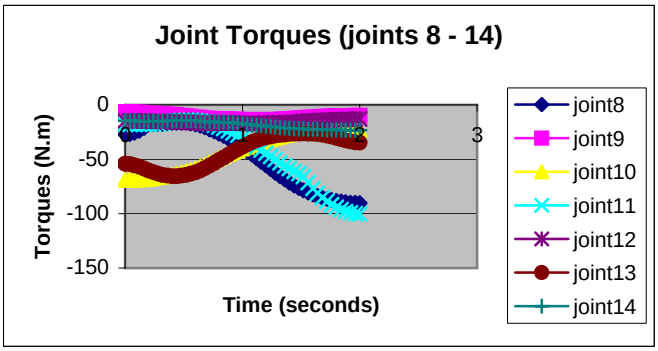

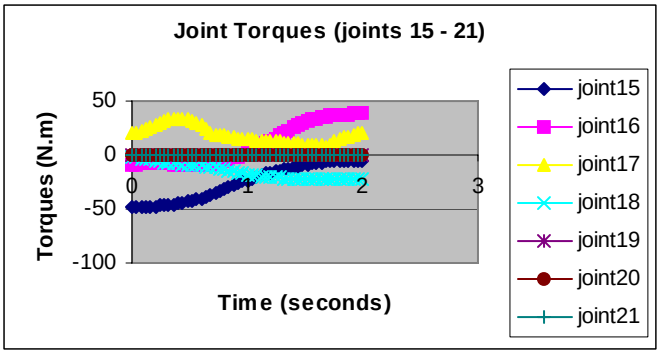

Fig. 9. Joint torque profiles

(a) Initial posture (b) Final posture

Fig. 10. Visual demonstration

The musculoskeletal system is composed of the skeletal system and the skeletal muscles. This system of muscles and bones is arranged throughout the body as numerous levers where the bones act as the levers and the joints between them serve as fulcrums in Fig. 11, which shows some of the major muscles of the upper arm and illustrates how they are attached to the skeletal system.

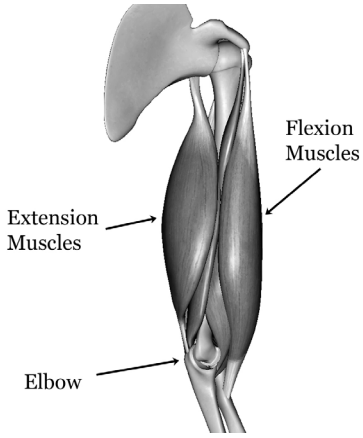

Fig. 11. Major muscles of the upper arm

Motion is then created by the muscles pulling on the bone to create torque about a joint. Since muscles can only act in tension, each joint requires one set of muscles to create a positive torque and a separate set to create negative torque. In Fig. 11, the elbow extension and flexion muscles are identified. Based on the joint torque torque results in the previous section, we have developed an optimization-based method to determine muscle forces.

MECHANICAL SYSTEM

Consider the simple one muscle model shown in Fig. 12, which represents the medial head of the bicep. This muscle originates on the scapula and inserts below the elbow on the radius. For this simple example, only the torque created at the elbow will be considered. When the muscle is activated, it creates a force on the radius. For this simple example it will be assumed that this force points at the muscle origin. This force creates a torque about the elbow by acting on a moment arm that lies along the radius (Fig. 13).

This force can be resolved into two components; the rotational component which is normal to the moment arm, and the stabilizing component which is parallel to the moment arm (Fig. 14). The rotational component is the portion of the force which actually contributes to joint torque. It is important to note that as the joint angle changes, so does the rotational component (Fig. 15). So, the resulting torque is not only a function of the muscle force, but also the current joint angle.For this simple one-muscle example, determining the muscle force needed to achieve a desired torque at a specific joint angle is simple. Torque is found with $\mathbf{T} = \mathbf{r} \times \mathbf{F}$, where $\mathbf{T}$ is torque, $\mathbf{r}$ is a vector pointing from the joint to the point where the muscle acts on the bone and $\mathbf{F}$ is the force. Unfortunately, once more muscles are added to this problem, it is no longer trivial to solve. To illustrate this, Fig. 16 shows two more muscles added to the previous example.

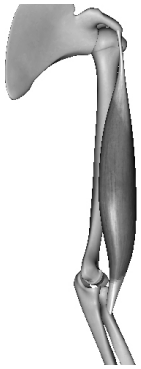

Fig. 12. Medial Bicep Brachii

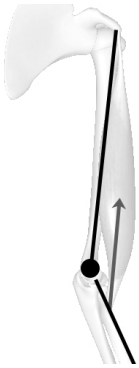

Fig. 13. Force from Bicep

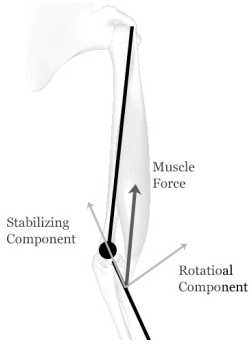

Fig. 14. Muscle force components

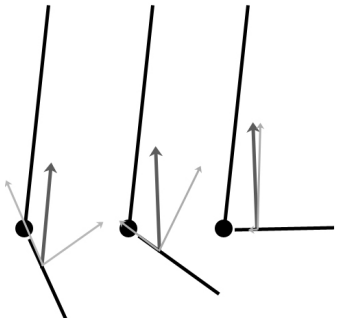

Fig. 15.Effect of joint angle

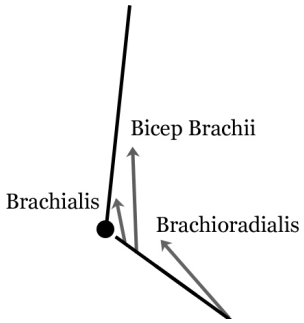

Fig. 16 Three muscles acting on the lower arm

Using the same equation, torque is found with $\mathbf{T} = \mathbf{r}_b \times \mathbf{F}_b + \mathbf{r}_{bc} \times \mathbf{F}_{bc} + \mathbf{r}_{br} \times \mathbf{F}_{br}$, where *b* denotes Bicep, *bc* denotes the Brachialis, and *br* denotes the Brachioradialis. Finding the muscle forces to achieve a desired torque at a specified angle becomes an indeterminate problem because there is one equation with three unknowns ($\mathbf{F}_b$, $\mathbf{F}_{bc}$, and $\mathbf{F}_{br}$). To solve this problem, optimization must be used.

OPTIMIZATION

Solving this problem with optimization requires a cost function which will be minimized while obeying various constraints. There have been many cost functions proposed, and choosing the most appropriate function is likely dependent on the situation. For example, quick movement to avoid a collision will probably require a different cost function than a movement that needs to be precise and smooth. Many common cost functions use muscle activation as variables. Muscle activation is a value that ranges between 0 and 1 where 0 indicates no muscle activation and 1 indicates a fully activated muscle. Muscle force can then be defined as $F = a * F_{\max}$ where a is the activation and $F_{\max}$ is the maximum theoretical force that muscle can generate, which is calculated by the muscle's physical cross sectional area. Torque can now be represented as $\mathbf{T} = \mathbf{r} \times (a * \mathbf{F}_{\max})$. To simplify the problem, only the torque being generated about the rotational axis of the elbow will be considered. This allows the torque equation to become $T = r * a * F_{max}$ where *r* is a constant and F_{max} is the rotational component of $\mathbf{F}_{max}$. This problem can now be solved with the following optimization formulation where *n* is the number of muscles.

Find: $a_1, a_2, \ldots, a_n$

to minimize: $$J = \sum_{i=1}^{n} a_i^2$$

subject to: $$T = \sum_{i=1}^{n} r_i (a_i F_{i\max}) \qquad (4)$$

$$0 \le a_i \le 1$$

Note that by simply adding more torque equation constraints, this formulation can be extended to cover numerous joints.

For this example, ten muscles that are used to flex/extend the forearm and pronate/supinate the hand will be considered. These muscles are the brachialis, brachioradialis, bicep long, bicep short, tricep lateral, tricep long, tricep medial, pronator teres, supinator, and anconeus. Torque about the elbow and the pronating axis of the wrist are given and the orientation of these joints is known. The objective is to find the muscle activation level of the ten muscles listed above. This will be accomplished through optimization as described in

the previous section. For this example, the problem is formulated as follows:

Find: $a_1 \ldots a_{10}$

to minimize: $J = \sum_{i=1}^{10} a_i^2$

subject to: $T_{BR} + T_{BL} + T_{BS} + T_{PT} + T_{SUP} = 1$

$$T_{BR} + T_{BCH} + T_{BL} + T_{BS} + T_{TLAT} + T_{TLON} + T_{TM} + T_{PT} + T_{SUP} + T_{ANC} = 10$$

$$0 \le a_i \le 1$$

where T_x is the torque generated by that muscle. Note that for this problem, it is given that the torque about the wrist is 1 Nm and the torque about the elbow is 10 Nm. It should also be noted that while all the muscle considered contribute some torque to the elbow, only five contribute torque to the wrist.

Next the torque generated by each muscle must be calculated. These are calculated as

$$T_i = r_i x_i a_i F_{i\max}$$

where *r* is the moment arm, *x* is the rotational component of the unit vector representing the force line, *a* is the activation level, and F_{max} is the theoretical maximum isotonic force which that muscle can create. The maximum isotonic force can be calculated by multiplying the maximum physiological achievable muscle stress (600 kPa) to the physiological cross sectional area (PSCA) of the muscle (Berme *et al*, 1987). The torque equation can then be represented as

$$T_i = r_i x_i a_i PSCA_i * 600$$

Note that *r* and *PSCA* are constants while *x* is dependent on the joint angles and *a* is the design variable. Since the joint angles are known, *x* can be calculated from geometry while *r* and *PSCA* can be found in the literature (Maurel and Thalman, 1998). For example, T_{BR} about the elbow can be calculated as

$$T_{BR} = 0.0662 * 0.424 * a * 4.70 * 600 = 14.149a$$

So, for the given orientation, the constraint equations can be calculated as

$$0.002a_2 + 1.281a_3 + 1.112a_4 + (-0.724)a_8 + 0.025a_9 = 1$$

$$14.149a_1 + 8.670a_2 + 4.833a_3 + 4.228a_4 + (-2.640)a_5 + (-2.617)a_6$$

$$+(-2.636)a_7 + 1.230a_8 + 4.012a_9 + 0.0112a_{10} = 10$$

Solving the optimization problem predicts the following activation levels for each muscle: Bracialis 0.303, Brachioradialis 0.186, Bicep Long 0.445, Bicep Short 0.384, Tricep Lateral 0, Tricep Long 0, Tricep Medial 0, Pronator Teres 0, Supinator 0.093, Anconeus 0.

MUSCLE STRESS

Muscle forces obtained in the previous section are not enough to show all aspects of muscle injury. Muscle stress is one important index for muscle injury. Several major methods have been proposed for physically based deformable modeling (Gibson and Mirtich 1997): mass-spring models, finite element methods, finite volume models (Teran *et al,* 2003), and other low-degree approximated continuum models. There are essentially two issues in deformable body modeling: how to parameterize a body and how to bring in physical behavior to the system.

Biomechanical analysis of skeletal muscles is an important task in the development of a digital human system. The stress level within the muscle of action is particularly of interest to us. However, the stress analysis with the finite element method is usually intensive with dense mesh as a result of irregular shapes of muscles. Considering the variety of muscle shapes and functionality differences, simulations with over simplified or idealized muscle geometry and biomechanics will not give satisfactory results, especially when trying to exam a group of cooperating muscles in action.

In our work, a new modeling method (Zhou and Lu 2005) is being developed to overcome the difficulties of computation intensity of the standard finite element method in an interactive virtual environment. The method is based on the combination of Non-Uniform Rational B-spline (NURBS) geometric representation and the Galerkin finite element methods, which intuitively bridges the two of them without the meshing procedure and hence with low degrees of freedom.

We use the NURBS geometry to represent the shape of muscles in order to capture the complexity of muscle geometry. The muscle shape can be extracted from medical image data such as the Visible Human Data Set (U.S. National Library of Medicine). Our method requires further extension of NURBS surface to NURBS solid, which keeps the geometric information of surface while extending to the inside. The NURBS solid representation can be written as

$$\mathbf{P}(u,v,w) = \sum_{i=0}^{n}\sum_{j=0}^{m}\sum_{k=0}^{l} \mathbf{P}_{i,j,k} R_{i,j,k}(u,v,w)$$

Using the isoparametric mapping technique, the NURBS geometric shape functions are used as the interpolation functions of finite elements. Therefore, the displacement mapping can be written as

$$\mathbf{d}(u,v,w) = \sum_{i=0}^{n}\sum_{j=0}^{m}\sum_{k=0}^{l} \mathbf{d}_{i,j,k} R_{i,j,k}(u,v,w)$$

where $\mathbf{d}_{i,j,k}$ is the displacement of the control point $\mathbf{P}_{i,j,k}$.

Based on the above-established mapping, we can calculate the deformation gradient and other needed quantities for the finite element computation. Because muscles are general under very large deformation during human motions, a fully nonlinear formulation for the analysis of large-strain motion of muscle is used.

CONSTITUTIVE MODEL OF SKELETAL MUSCLE

The internal structure of skeletal muscle is comprised of soft tissues with various material properties. More important, skeletal muscles are active and the properties

of the active tissue are altered upon activation. In our work, the muscle model is described by a hyperelastic, anisotropic constitutive equation that includes an active component.

The hyperelastic strain energy function is assumed to be the sum of two parts: energy function of the passive ground substance and active fibrous structure. The passive ground substance consists of connective tissue, water, etc, and is modeled as isotropic neo-Hookean material. The muscle fiber strain energy is assumed to be a function of the muscle fiber stretch and the muscle activation level. The muscle fiber directions are generally distributed with different patterns among different muscles. In our work, we used the isocurves of the NURBS solid to model the muscle fibers and its directions.

RESULTS OF MUSCLE STRESS

The motion analysis provides at discrete points of time the joint positions and rotations as well as the activation level in individual muscles. From the position of bones, the displacement boundary conditions for the muscles can be known. And the activations of muscles are fed into the constitutive model. The stress analysis is then conducted using the NURBS-FEM developed. As shown in figure 1, both passive and active motions of muscles are simulated, and the corresponding muscle deformations and stresses can be obtained.

Using the pseudo-static simulation of muscle deformation at discrete points of time, the muscle force-extension curves are shown in Fig. 17 with different length changes. The curves (Fig. 18) show a behavior that qualitatively matches what is reported in the literature (Zajac 1989). It can be seen that, with the same length, the active muscle generates more force than the passive one, and the largest active muscle force generated happens at the initial rest length of muscle.

SUMMARY AND DISCUSSION

This paper presents the new capabilities of the virtual human (Santos™). These new capabilities include hand modeling, advances in posture prediction (new vision objective function, multiple end-effectors, advanced inverse kinematics (IK), self-collision avoidance), dynamic motion prediction, and musculoskeletal modeling (optimization-based method to determine muscle forces and NURBS-FEM approach for muscle stress).

In addition to the above-mention newly developed capabilities, exciting research is still on-going and concerns more features for Santos™. Particle and FEM methods are implemented to clothing modeling. Ingress/egress is studied using motion capture system and a swing dynamic prediction model is being developed. Collision avoidance is being extended from self collision-free to environment collision avoidance. Finally, a user- friendly interface is being developed.

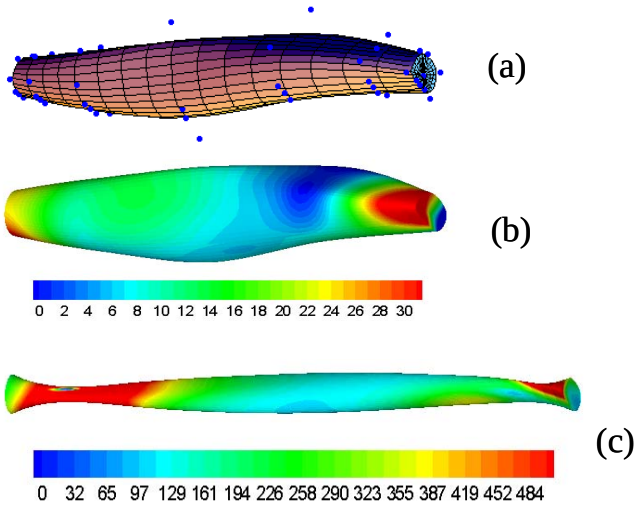

Fig. 17. Stress analysis of muscle. (a) initial rest geometry (b) active contraction (c) large passive deformation.

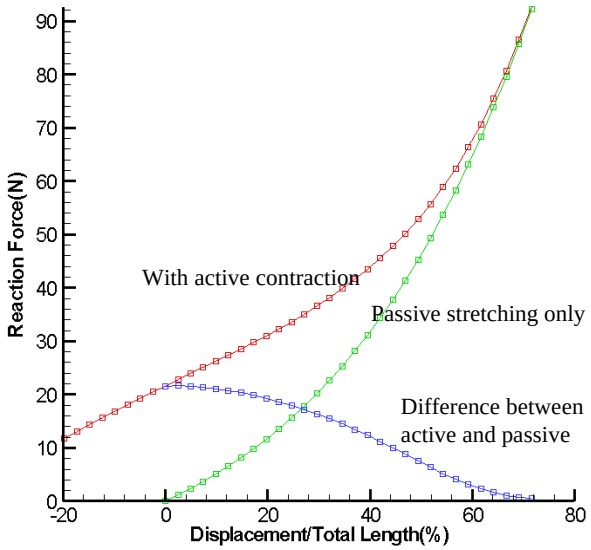

Fig. 18. Force-extension curve

ACKNOWLEDGEMENTS

This research is funded partly by the US Army TACOM project: Digital Humans and Virtual Reality for Future Combat Systems (FCS) (DAAE07-03-D-L003) and Caterpillar Inc. project: Digital Human Modeling for Safety and Serviceability.

REFERENCES

1. Beck, D.J. and Chaffin, D.B., 1992, “An evaluation of inverse kinematics models for posture prediction”, *Computer Applications in Ergonomics, Occupational Safety and Health*, Elsevier, Amsterdam, The Netherlands, pp. 329-336.
2. Berme, N., Heydinger, G., and Cappozzo, A., “Loads Transmitted at the Anatomical Joints”. In A. Morechi (ed) *Biomechanics of Engineering: Modeling, Simulation, Control*, Wien, New York, 1987.
3. Chaffin, D.B., 1997, “Development of computerized human static strength simulation model for job design”, Human Factors and Ergonomics in Manufacturing, Vol. 7, pp. 305-322
4. Das, B. and Behara, D.N., 1998, “Three-dimensional workspace for industrial workstations”, *Human Factors*, Vol. 40, No. 4, pp. 633-646.
5. Faraway, J.J., Zhang, X.D., and Chaffin, D.B., 1999, “Rectifying postures reconstructed from joint angles to meet constraints”, *Journal of Biomechanics*, Vol. 32, pp. 733-736.
6. Farrell, K., Marler, R. T., and Abdel-Malek, K. (2005), "Modeling Dual-Arm Coordination for Posture: An Optimization-Based Approach", *SAE Human Modeling for Design and Engineering Conference*, June, Iowa City, IA, Society of Automotive Engineers, Warrendale, PA.
8. Gill, P., Murray, W., and Saunders, A, 2002, “SNOPT: An SQP algorithm for large-scale constrained optimization,” *SIAM Journal of Optimization*, Vol. 12, No. 4, pp. 979-1006.
9. Hase, K., Yamazaki, N., 1997, “Development of three-dimensional whole-body musculoskeletal model for various motion analyses”, *JSME International Journal*, Series C, Vol. 40 no. 1, pp. 25-32.
10. Jung, E.S. and Choe, J., 1996, “Human reach posture prediction based on psychophysical discomfort”, *International Journal of Industrial Ergonomics*, Vol. 18, pp. 173-179.
11. Jung, E.S., Kee, D., and Chung, M.K., 1992, “Reach posture prediction of upper limb for ergonomic workspace evaluation**”,** *Proceedings of the 36th Annual Meeting of the Human Factors Society*, Atlanta, GA, Part 1, Vol. 1, pp. 702-706.
12. Jung, E.S., Kee, D., and Chung, M.K., 1995, “Upper body reach posture prediction for ergonomic evaluation models”, *International Journal of Industrial Ergonomics,* Vol. 16, pp. 95-107.
13. Kee, D., Jung, E.S., and Chang, S., 1994, “A man-machine interface model for ergonomic design”, *Computers & Industrial Engineering*, Vol. 27, pp. 365-368.
14. Kim, J., Abdel-Malek, K., Mi, Z., and Nebel, K., 2004, “Layout design using an optimization-based human energy consumption formulation”, SAE Digital Human Modeling for Design and Engineering, June 15-17, Rochester, Michigan, USA.
15. Kim, J.O., Khosla P.K. 1992: Real-Time Obstacle Avoidance Using Harmonic Potential Functions. *IEEE Transactions on Robotics and Automation.* **8**(3), 338-349.
16. Kuffner, J., Nishiwaki, K., Kagami, S., Kuniyoshi, Y., Inaba, M., Inoue, H. 2002, “Self-collision detection and prevention for Humanoid Robots”, *In Proc. 2002 IEEE Int’l Conf. on Robotics and Automation (ICRA 2002)*, Washington, DC., May 2002, 2265-2270.
17. Marler, R. T., Yang, J., Arora, J. S., and Abdel-Malek, K. (2005a), “Study of Bi-Criterion Upper Body Posture Prediction using Pareto Optimal Sets”, *IASTED International Conference on Modeling, Simulation, and Optimization*, August, Oranjestad, Aruba, International Association of Science and Technology for Development, Canada.
18. Marler, R. T., Rahmatalla, S., and Shanahan, M., and Abdel-Malek, K. (2005b), "A New Discomfort Function for Optimization-Based Posture Prediction", *SAE Human Modeling for Design and Engineering Conference*, June, Iowa City, IA, Society of Automotive Engineers, Warrendale, PA.
19. Maurel, W. and Thalman, D., *A Case Study on Human Upper Limb Modelling for Dynamic Simulation,*http://ligwww.epfl.ch/~maurel/CMBBE98.html>
20. Ozaki, H., Mohri, A., 1986, “Planning of collision-free moments of a manipulator with dynamic constraints”, *Robotica.* **4**, 163-169.
21. Savescu, A.V., Cheze, L., Wang, X., Beurier, G., and Verriest, J. P., A 25 degrees of freedom hand geometrical model for better hand attitude simulation. SAE International*,* 2004-01-2196.
22. Teran, J., Blemker, S., Ng-Thow-Hign, V., and Fedkiw, R. 2003, “Finite volume method for the simulation of skeletal muscle”, *In Proc. of the 2003 SIGGRAPH/Eurographics Symp. on Computer Animation*, 68-74.
23. U.S. National Library of Medicine. The visible human project, 1994. http://www.nlm.nih.gov/research/visible/.
24. Yang, J., Marler, R. T., Kim, H. J., Farrell, K., Mathai, A., Beck, S., Abdel-Malek, K., Arora, J. S., and Nebel, K. (2005), "Santos: A New Generation of Virtual Humans", *SAE 2005 World Congress*, April, Detroit, MI, Society of Automotive Engineers, Warrendale, PA.
25. Zajac, F.E. Muscle and tendon: properties, models, scaling, and application to biomechanics and motor control. Critical Reviews in Biomedical Engineering, 17, 359-411, 1989.
26. Zhou, X. and Lu, J. 2005. NURBS-based Galerkin method and application to skeletal muscle modeling. In Proceedings of the 2005 ACM Symposium on Solid and Physical Modeling (Cambridge, Massachusetts, June 13 - 15, 2005). SPM '05. ACM Press, New York, NY, 71-78.

CONTACT

Dr. Jingzhou Yang, Virtual Soldier Research (VSR) Program, Center for Computer-Aided Design, The University of Iowa, Iowa City, IA 52242, Tel: 319-353-2249, Fax: 319-384-0542,
E-Mail: jyang@engineering.uiowa.edu.